

Fermionic fluctuation corrections to bubble nucleation

J. Baacke¹ and A. Sürig²

Institut für Physik, Universität Dortmund
D - 44221 Dortmund , Germany

Abstract

We determine the fermionic corrections to the nucleation rate of bubbles at the electroweak phase transition. The fermion determinant is evaluated exactly and by using the gradient expansion. The gradient expansion is found to be a reliable approximation and is used to extrapolate to the large values of $\nu_n = (2n + 1)\pi T$ needed in the Matsubara sum. The contribution to effective action is found to be negative and to be given, essentially, by the gradient terms, the finite part of the wave function renormalization. Only the top quark contribution is evaluated, it is of the same order as the Higgs- and W-boson contributions found previously, but of opposite sign.

¹ e-mail: baacke@het.physik.uni-dortmund.de

²e-mail: suerig@het.physik.uni-dormund.de

1 Introduction

The physics of the electroweak phase transition has been discussed recently in various aspects [1]. Many subjects, as e.g. the question of baryogenesis [2, 3] are still controversial [4, 5]. Even the nature of the phase transition is not known at present. The temperature dependence of the effective potential has been studied in perturbation theory [6, 7] as well as in lattice simulations [8, 9]. If the mass of the Higgs is not too high (less than M_W) the phase transition is supposed to be first order [10]. In this case the transition from the symmetric vacuum with massless particles to the broken symmetry phase would proceed via bubble nucleation. This phenomenon as well as its cosmological aspects, has been studied by various groups [11, 12, 13].

Part of the basic information needed in developing the bubble formation and expansion scenario is the determination of their nucleation rate. In the small temperature span of 1 GeV in which the phase transition takes place bubbles of various sizes can be formed. Their nucleation rate varies over several orders of magnitude. The basic rate is determined [14, 15, 16] by the classical minimal bubble action. Its exponential is the tunneling rate. The semiclassical reaction rate includes, however, also preexponential factors, the fluctuation determinants, determined by the fluctuation of W boson, Higgs and fermion fields in the background of the minimal bubble profile. The bosonic fluctuations have been computed recently [17, 18] and found to yield sizeable suppression factors, the one-loop effective action (or equivalently the free energy divided by the temperature) being of the same order as the classical bubble action. In the high temperature theory, obtained by retaining only the Matsubara frequency 0, fermions do not contribute. However, recent determinations of the fermionic contribution to the sphaleron rate [19] let us expect that at least the top quark will influence the transition rate in an essential way. Of course we have to perform such a computation in the four-dimensional finite temperature quantum field theory, i.e. by summing over all Matsubara frequencies.

The plan of this paper is as follows: in the next section we will introduce the model and set up the basic relations for the bubble nucleation rate. The fermion determinant is defined in section 3. In section 4 we will discuss the leading terms, of first and second order in the external field vertex function. Part of their contribution is contained already in the effective potential and should not be included again. This renders the discussion in that section very lengthy and pedantic. In section 5 we present the computation of the finite higher order contributions to fermionic effective action. The results of an exact numerical computation are compared with an analytic approximation based on the gradient expansion. The latter one is used, then, to obtain the actual results which are presented and discussed in section 6.

2 Basic relations

As a basis for the computation of fluctuations we need an action which describes the nucleation of minimal bubbles and which can be used to compute the bubble profiles. This must necessarily be a finite temperature action which describes the essential features of the phase transition. We will be using here an action obtained in the electroweak theory by evaluating the one-loop effective potential à la Coleman-Weinberg [20]. This has been computed by various authors [21, 22, 23]; here we use the formulation of Dine et al. [13]. The finite temperature action was found by these authors - for the temperatures relevant to the phase transition - to be well represented by its high temperature limit. Though we will compute the fermion determinant at finite temperature, it should be a good approximation to compute the bubble profile from this approximate action the more so as the one-loop corrections will be computed exactly and their contribution to the approximate one-loop effective potential will be subtracted at the end in order to avoid double-counting (see below). This way of determining the ‘classical’ profile from an action including already one-loop corrections has been discussed critically by Weinberg [24]; we think that this intermediate approach nevertheless yields relevant information, namely the order of magnitude and sign of the corrections as well as their structure and relative importance.

The basic Euclidean finite temperature action then given by ³

$$S_{\text{ft}} = \int_0^\beta d\tau \int d^3x \left[\frac{1}{2} (\partial_\mu \Phi)^\dagger (\partial_\mu \Phi) + V_{ht}(\Phi^\dagger \Phi) \right] + S_F. \quad (2.1)$$

Φ is the complex doublet of Higgs fields. Here this field will always occur as a background field describing the minimal bubble. It can be parametrized then as

$$\Phi(\vec{x}) = v_0 \Phi(\vec{x}) \begin{pmatrix} 0 \\ 1 \end{pmatrix}. \quad (2.2)$$

V_{ht} is the high temperature potential which includes the one-loop effective potential in the high temperature approximation

$$V_{\text{ht}}(\Phi^\dagger \Phi) = D(T^2 - T_0^2) \Phi^\dagger \Phi - ET \Phi^\dagger \Phi^{3/2} + \frac{\lambda_T}{4} \Phi^\dagger \Phi^2. \quad (2.3)$$

Its parameters are given - for $\Theta_w = 0$ - by

$$\begin{aligned} D &= (3m_W^2 + 2m_t^2)/8v_0^2 \\ E &= 3g^3/32\pi \\ B &= 3(3m_W^4 - 4m_t^4)/64\pi^2 v_0^4 \\ T_0^2 &= (m_H^2 - 8v_0^2 B)/4D \end{aligned} \quad (2.4)$$

$$\lambda_T = \lambda - 3(3m_W^4 \ln \frac{m_w^2}{a_B T^2} - 4m_t^4 \ln \frac{m_t^2}{a_F T^2})/16\pi^2 v_0^4 \quad (2.5)$$

³ We leave out the gauge fields here, since they do not appear in the bubble background field configuration and since we are not going to compute their fluctuation determinant.

with $\ln a_B = 2 \ln 4\pi - 2\gamma$ and $\ln a_F = 2 \ln \pi - 2\gamma$.

For $T > T_0$ the potential has a minimum at $|\Phi| = 0$ corresponding to the symmetric phase and a second minimum at

$$|\Phi| = \tilde{v}(T) = \frac{3ET}{2\lambda} + \sqrt{\left(\frac{3ET}{2\lambda}\right)^2 + v^2(T)} \quad (2.6)$$

where

$$v^2(t) = \frac{2D}{\lambda_T}(T_0^2 - T^2). \quad (2.7)$$

This minimum is degenerate with the one at $\Phi = 0$ at a temperature defined implicitly by

$$T_C = T_0 / \sqrt{1 - E^2 / D\lambda_{T_C}}. \quad (2.8)$$

T_C marks the onset of bubble formation by thermal barrier transition.

The fermion action S_F can be written - for vanishing gauge fields and for Higgs field configurations of the form (2.2) - in terms of four-component Dirac spinors as

$$S_F = \int_0^\beta d\tau \int d^3x \left[\sum_f (\bar{\psi}^f \gamma_\mu \partial_\mu \psi^f) - \sum_{ff'} g_Y^{ff'} v_0 \Phi \bar{\psi}^f \psi^{f'} \right] \quad (2.9)$$

where the Yukawa couplings are related to the fermion mass matrix via $g_Y^{ff'} v_0 = m^{ff'}$. The sum over f is over flavors and colors. Here we will consider only the contribution of the top quark. This has been done already in the high temperature action given above for the reason that its contribution is much larger than the one of lighter quark and lepton fields. This will also be the case for the exact one-loop action.

The process of bubble nucleation is - within the approach of Langer [14] and Coleman and Callan [15, 16], followed by the work of Affleck [25], Linde [26] and others - described by the rate

$$\Gamma/V = \frac{\omega_-}{2\pi} \left(\frac{\tilde{S}}{2\pi}\right)^{3/2} \exp(-\tilde{S}) \left(\frac{\mathcal{J}_F}{\mathcal{J}_B}\right)^{1/2}. \quad (2.10)$$

Here \tilde{S} is the high-temperature action, Eq. (2.1), with the new rescaling, minimized by a classical τ independent minimal bubble configuration (see below). $\mathcal{J}_{F/B}$ are the fermionic and bosonic fluctuation determinants which describe the next-to-leading part of the semiclassical approach. \mathcal{J}_F - whose computation is the

aim of this work - will be defined below; its logarithm is related to the fermionic one-loop effective action by

$$S_{\text{eff}}^F = -\frac{1}{2} \ln \mathcal{J}_F . \quad (2.11)$$

Finally ω_- is the absolute value of the unstable mode frequency.

The classical bubble configuration is described by a vanishing gauge field and a real τ independent spherically symmetric Higgs field. For the bubble configuration we make the Ansatz

$$\Phi(\vec{x}) = \tilde{v}(T)\phi(r) \begin{pmatrix} 0 \\ 1 \end{pmatrix} \quad (2.12)$$

where we have rescaled Eq. (2.2) via $v_0\Phi(r) = \tilde{v}(T)\phi(r)$. In all our numerical computations we will use the scale $(g_w\tilde{v}(T))^{-1}$ for the coordinates. Defining the rescaled high temperature potential as

$$\tilde{V}_{ht} = \frac{\lambda_T}{4g^2} \left[\phi^4 - \epsilon\phi^3 + \left(\frac{3}{2}\epsilon - 2\right)\phi^2 \right] \quad (2.13)$$

with

$$\epsilon = \frac{4ET}{\lambda_T\tilde{v}(T)} = \frac{4}{3} \left(1 - \frac{v^2(T)}{\tilde{v}(T)^2} \right) \quad (2.14)$$

and the high temperature coupling

$$\tilde{g}_3^2(T) = \frac{g_w T}{\tilde{v}(T)} \quad (2.15)$$

the bubble action is given by

$$\tilde{S} = \frac{4\pi}{\tilde{g}_3^2(T)} \int_0^\infty r^2 dr \left[\frac{1}{2} \left(\frac{d\phi}{dr} \right)^2 + \tilde{V}_{ht}(\phi) \right] . \quad (2.16)$$

It is minimized if $\phi(r)$ is a solution of the associated Euler-Lagrange equation

$$-\phi''(r) - \frac{2}{r}\phi'(r) + \frac{d\tilde{V}_{ht}}{d\phi(r)} = 0 \quad (2.17)$$

with the boundary conditions

$$\lim_{r \rightarrow \infty} \phi(r) = 0 \quad \text{and} \quad \phi'(0) = 0 . \quad (2.18)$$

The bubble configuration varies from small thick wall bubbles to large thin wall bubbles in the narrow range ($\simeq 1$ GeV) between T_0 and T_C , both of order 100 GeV. We will use the variable

$$y = 3(1 - \epsilon/2) , \quad 0 < y < 1 \quad (2.19)$$

instead of T to parametrize this range of temperatures.

3 The fermionic fluctuation determinant

The fermionic action S_F of quarks can be rewritten in four component Dirac notation and for time-independent background configurations as

$$S_F = \int_0^\beta d\tau \int d^3x \bar{\psi} (\gamma_\mu \partial_\mu - m(\vec{x})) \psi \quad (3.1)$$

$$= \int_0^\beta d\tau \int d^3x \psi^\dagger (\partial/\partial\tau - H) \psi \quad (3.2)$$

where $m(\vec{x}) = g_Y \tilde{v}(T) \phi(r)$ and

$$H = \gamma^0 (-i\vec{\gamma}\vec{\nabla} + m(\vec{x})). \quad (3.3)$$

The field fluctuations are subject to antiperiodic boundary conditions at $\tau = 0$ and $\tau = \beta$, i.e.

$$\psi(\vec{x}, \beta) = -\psi(\vec{x}, 0) \quad (3.4)$$

which determines their frequencies to be the Matsubara frequencies $\nu_n = (2n + 1)\pi T$ with integer n , $-\infty < n < \infty$. Integrating out the fermion field leads to the fermionic prefactor

$$\mathcal{J}_F^{1/2} = \frac{\prod_{n\alpha} (i\nu_n + \omega_\alpha)}{\prod_{n,\alpha} (i\nu_n + \omega_\alpha^0)} \quad (3.5)$$

where ω_α denotes the eigenvalues of H . Using the fact that these eigenvalues occur in pairs $\pm\omega_\alpha$ we can rewrite this as

$$\mathcal{J}_F = \left(\frac{\prod_{n\alpha} (\nu_n^2 + \omega_\alpha^2)}{\prod_{n,\alpha} (\nu_n^2 + (\omega_\alpha^0)^2)} \right). \quad (3.6)$$

The fermion contribution to the effective action is therefore given by

$$S_{\text{eff}}^F = -\frac{1}{2} \ln \mathcal{J}_F = -\frac{1}{2} \sum_{n=-\infty}^{\infty} \ln \det \left(\frac{\nu_n^2 + \mathcal{M}}{\nu_n^2 + \mathcal{M}^0} \right). \quad (3.7)$$

Here $\nu_n = (2n + 1)\pi T$, the fluctuation operators \mathcal{M} and \mathcal{M}^0 are defined as

$$\begin{aligned} \mathcal{M} &= H^2 = -\Delta + \mathcal{V}(\vec{x}) \\ \mathcal{M}^0 &= (H^0)^2 = -\Delta \end{aligned} \quad (3.8)$$

and

$$\mathcal{V} = \begin{Bmatrix} m^2(\vec{x}) & -i\vec{\sigma}\vec{\nabla}m(\vec{x}) \\ i\vec{\sigma}\vec{\nabla}m(\vec{x}) & m^2(\vec{x}) \end{Bmatrix}. \quad (3.9)$$

A method for computing such fluctuation determinants numerically has been described recently [27]. Before we discuss the numerical part of the computation we have to ensure that the quantities we are going to compute are finite. The

effective action as defined formally in Eq. (3.7) is divergent. This is easily seen by expanding it w. r. t. the potential \mathcal{V} . One generates then the series of Feynman graphs depicted in Fig. 1, of which the first and second order graph are divergent. We will see that our numerical method allows to separate these two graphs from the remaining series which can be computed exactly and is finite. The divergences of the two leading graphs are obviously those of ordinary perturbation theory. Their divergent parts can be cancelled by the counterterms of the $T = 0$ theory. This will be described in the next section, following the work of Refs. [28] and [13].

4 Renormalization

We note first that the effective potential is renormalized usually at $T = 0$ in such a way that the vacuum expectation value v_0 and the Higgs mass, i.e. the second derivative at the broken symmetry minimum, are kept at their physical values. This will determine the counterterms in the effective action. We will, on the other hand, expand the effective action around the symmetric vacuum defined by $\Phi = 0$. The discussion of renormalization - especially at finite temperature - is therefore somewhat cumbersome; we will follow all steps very explicitly, though this may seem somewhat pedantic.

In order to cover both kinds of expansion we rewrite the effective action as

$$S_{\text{eff}} = -\frac{1}{2} \ln \mathcal{J} = -\frac{1}{2} \sum_{n=-\infty}^{+\infty} \ln \left(\frac{\det(\nu_n^2 - \Delta + \mu_F^2 + \mathcal{U})}{\det(\nu_n^2 - \Delta + \mu_F^2)} \right) \quad (4.1)$$

where now $\mu_F = m_F = g_Y v_0$ if one expands around the $T = 0$ broken symmetry vacuum and $\mu_F = 0$ if one expands around the high temperature symmetric phase. The 4×4 matrix \mathcal{U} is then given by

$$\mathcal{U} = \mathcal{V} - \mu_F^2 = \begin{Bmatrix} m_F^2 \Phi^2 - \mu_F^2 & -im_F \vec{\sigma} \vec{\nabla} \Phi \\ im_F \vec{\sigma} \vec{\nabla} \Phi & m_F^2 \Phi^2 - \mu_F^2 \end{Bmatrix}. \quad (4.2)$$

The field Φ is normalized in such a way that it takes the value 1 if the Higgs field is at its $T = 0$ vacuum expectation value.

In the following we will discuss the contributions of first and second order in the external potential both at $T = 0$ with massive propagators and at large T with massless propagators. Anticipating that we work at finite temperature we replace the space-time integration by $\beta \int d^3x$. Furthermore, for the second order diagrams we separate space and loop momentum integration formally, though the external momentum q acts as an operator in x space. This compact notation should not lead to confusion.

For the first order diagram at $T = 0$ we have

$$S_{\text{eff}}^{(1)}(\Phi, 0) = -\frac{1}{2}4\beta \int d^3x (m_F^2 |\Phi(x)|^2 - \mu_F^2) \int \frac{d^4p}{(2\pi)^4} \frac{1}{p^2 + \mu_F^2}. \quad (4.3)$$

Using a 4 - momentum cutoff Λ we get

$$S_{\text{eff}}^{(1)}(\Phi, 0) = -\frac{1}{8\pi^2}\beta \int d^3x (m_F^2 |\Phi(x)|^2 - \mu_F^2) (\Lambda^2 - \mu_F^2 \ln(\Lambda^2/\mu_F^2)). \quad (4.4)$$

Before we dispose further by introducing appropriate counterterms we turn to the second order contribution at $T = 0$. We have to evaluate

$$\begin{aligned} S_{\text{eff}}^{(2)}(\Phi, 0) &= \frac{1}{4}4\beta \int d^3x ((m_F^2 |\Phi(x)|^2 - \mu_F^2)^2 + m_F^2 |\nabla\Phi(x)|^2) \\ &\times \int \frac{d^4p}{(2\pi)^4} \frac{1}{p^2 + \mu_F^2} \frac{1}{(p+q)^2 + \mu_F^2}. \end{aligned} \quad (4.5)$$

A standard computation, using again a 4-momentum cutoff Λ leads to

$$\begin{aligned} S_{\text{eff}}^{(2)}(\phi, 0) &= \frac{1}{16\pi^2}\beta \int d^3x ((m_F^2 |\Phi(x)|^2 - \mu_F^2)^2 + m_F^2 |\nabla\Phi|^2) \\ &\times (\ln\left(\frac{\Lambda^2}{\mu_F^2}\right) - 1 - \int_0^1 d\alpha \ln(1 + \frac{q^2}{\mu_F^2}\alpha(1-\alpha))). \end{aligned} \quad (4.6)$$

Putting this together with the first order contribution and requiring all corrections to the potential and the wave function renormalization to vanish at $q^2 = 0$ we find that we need a counterterm

$$\begin{aligned} S_{\text{eff}}^{\text{c.t.}} &= \frac{\Lambda^2}{8\pi^2}\beta \int d^3x (m_F^2 (|\Phi(x)|^2 - 1)) \\ &- \frac{1}{16\pi^2} (\ln\left(\frac{\Lambda^2}{m_F^2}\right) - 1) \beta \int d^3x (m_F^4 (|\Phi(x)|^4 - 1) + m_F^2 |\nabla\Phi(x)|^2) \\ &- \frac{1}{8\pi^2} m_F^4 \beta \int d^3x (|\Phi(x)|^2 - 1). \end{aligned} \quad (4.7)$$

If the first and second order diagram are evaluated in the symmetric vacuum we find

$$\begin{aligned} S_{\text{eff}}^{(1+2,S)}(\Phi, 0) &= -\frac{\Lambda^2}{8\pi^2}\beta \int d^3x m_F^2 |\Phi(x)|^2 + \frac{1}{16\pi^2} (\ln\left(\frac{\Lambda^2}{q^2}\right) + 1) \\ &\times \beta \int d^3x (m_F^4 |\Phi(x)|^4 + m_F^2 |\nabla\Phi(x)|^2). \end{aligned} \quad (4.8)$$

Leaving out the field-independent terms - which are due to a difference in the vacuum energy density - we get

$$\begin{aligned} S_{\text{eff}}^{(1+2,S)}(\Phi, 0) + S_{\text{eff}}^{\text{c.t.}} &= -\frac{1}{16\pi^2} (\ln\left(\frac{q^2}{\mu_F^2}\right) - 2) \beta \int d^3x (m_F^2 |\Phi(x)|^4 + m_F^2 |\nabla\Phi(x)|^2) \\ &- \frac{1}{8\pi^2} \mu_F^2 \beta \int d^3x m_F^2 |\Phi(x)|^2 \end{aligned} \quad (4.9)$$

which is to be evaluated with the background profile. The last term is already contained in the high temperature potential (2.3), it occurs in the coefficient $-DT_0^2 = -(m_H^2 - 8v_0^2 B)/4$ via the top contribution to B .

Turning now to the first order diagram at finite temperature we have to evaluate

$$S_{\text{eff}}^{(1)}(\Phi, T) = -\frac{1}{2}4\beta \int d^3x (m_F^2 |\Phi(x)|^2 - \mu_F^2) T \sum_{n=-\infty}^{+\infty} \int \frac{d^3p}{(2\pi)^3} \frac{1}{\nu_n^2 + \mu_F^2 + \mathbf{p}^2}. \quad (4.10)$$

In order to separate $T = 0$ and finite temperature contributions we use [28]

$$\begin{aligned} T \sum_{n=-\infty}^{\infty} \frac{1}{((2n+1)\pi T)^2 + \mathbf{p}^2 + \mu_F^2} \\ = \frac{1}{2E_F} - \frac{1}{E_F} \frac{1}{\exp(E_F/T) + 1} \end{aligned} \quad (4.11)$$

with $E_F = \sqrt{\mathbf{p}^2 + \mu_F^2}$. In the last line the second term vanishes as $T \rightarrow 0$, so the first one represents the $T = 0$ contribution which we have considered earlier. Inserting the second part into the expression for $\mathcal{J}^{(1)}$ we find the finite temperature part

$$\Delta S_{\text{eff}}^{(1)}(\Phi, T) = 2\beta \int d^3x (m_F^2 |\Phi(x)|^2 - \mu_F^2) \int \frac{d^3p}{(2\pi)^3} \frac{1}{E_F} \frac{1}{\exp(E_F/T) + 1}. \quad (4.12)$$

We have to evaluate this expression for a bubble in the symmetric vacuum where $\Phi \neq 0$ only locally and where $\mu_F = 0$ at spatial infinity. Then $E_F = |\mathbf{p}|$ and we find

$$\Delta S_{\text{eff}}^{(1)}(\Phi, T) = \frac{T^2}{12} m_F^2 \beta \int d^3x |\Phi(x)|^2. \quad (4.13)$$

This contribution is already taken into account in the T^2 term of the three dimensional high temperature action (2.1). Therefore the finite temperature part of the first order tadpole diagram has to be omitted entirely.

As the second order contribution at finite T we have to evaluate

$$\begin{aligned} S_{\text{eff}}^{(2)}(\Phi, T) &= \frac{1}{4}\beta \int d^3x 4(m_F^4 |\Phi(x)|^4 + m_F^2 |\nabla\Phi(x)|^2) \\ &\times T \sum_{n=-\infty}^{+\infty} \int \frac{d^3p}{(2\pi)^3} \frac{1}{(\nu_n^2 + \mathbf{p}^2)(\nu_n^2 + (\mathbf{p} + \mathbf{q})^2)}. \end{aligned} \quad (4.14)$$

Momentum integration and Matsubara frequency summation can be carried out via

$$T \sum_{n=-\infty}^{+\infty} \int \frac{d^3p}{(2\pi)^3} \frac{1}{(\nu_n^2 + \mathbf{p}^2)(\nu_n^2 + (\mathbf{p} + \mathbf{q})^2)} =$$

$$\begin{aligned}
& T \sum_{n=-\infty}^{+\infty} \int_0^1 d\alpha \int \frac{d^3 p}{(2\pi)^3} \frac{1}{(\nu_n^2 + \mathbf{p}^2 + \alpha(1-\alpha)\mathbf{q}^2)^2} = \\
& T \sum_{n=-\infty}^{+\infty} \int_0^1 d\alpha \int \frac{d^3 p}{(2\pi)^3} \frac{-d}{d(\mathbf{p}^2)} \frac{1}{\nu_n^2 + \mathbf{p}^2 + \alpha(1-\alpha)\mathbf{q}^2} = \quad (4.15) \\
& \frac{1}{\pi^2 T} \int_0^1 d\alpha \int \frac{d^3 p}{(2\pi)^3} \frac{-d}{d(\mathbf{p}^2)} \frac{\pi^2 T}{2E_\alpha} \tanh(E_\alpha/2T)
\end{aligned}$$

where $E_\alpha^2 = \mathbf{p}^2 + \alpha(1-\alpha)\mathbf{q}^2$. The $T = 0$ part may be recovered by performing the limit $T \rightarrow 0$. Subtracting this part we find for the finite temperature supplement

$$\begin{aligned}
& \int_0^1 d\alpha \frac{1}{2\pi^2} \int_0^\infty dp p^2 \frac{-d}{2pd} \frac{-1}{E_\alpha} \frac{1}{\exp(E_\alpha/T) + 1} = \quad (4.16) \\
& \int_0^1 d\alpha \frac{-1}{4\pi^2} \int_0^\infty \frac{dp}{E_\alpha} \frac{1}{\exp(E_\alpha/T) + 1}
\end{aligned}$$

so that

$$\begin{aligned}
\Delta S_{\text{eff}}^{(2)}(\Phi, T) &= -\frac{1}{4\pi^2} \beta \int d^3 x (m_F^4 |\Phi(x)|^4 + m_F^2 |\nabla \Phi(x)|^2) \quad (4.17) \\
&\times \int_0^1 d\alpha \int_0^\infty \frac{dp}{E_\alpha} \frac{1}{\exp(E_\alpha/T) + 1}.
\end{aligned}$$

Part of this term is already contained in the high temperature effective action. The momentum integral has been considered by Dolan and Jackiw [28]; it can be expanded to leading order in T , i.e. up to terms of order $1/T^2$ as

$$\int_0^\infty \frac{dp}{E_\alpha} \frac{1}{\exp(E_\alpha/T) + 1} = -\frac{1}{4} \left(\ln \left(\frac{\alpha(1-\alpha)q^2}{\pi^2 T^2} \right) + 2\gamma \right) + O(q^2/T^2) \quad (4.18)$$

If this is inserted into the previous equation we find

$$\begin{aligned}
\Delta S_{\text{eff}}^{(2)}(\Phi, T) &= \frac{1}{16\pi^2} \int_0^1 d\alpha \left(\ln \left(\frac{\alpha(1-\alpha)q^2}{\pi^2 T^2} \right) + 2\gamma \right) \quad (4.19) \\
&\beta \int d^3 x (m_F^4 |\Phi(x)|^4 + m_F^2 |\nabla \Phi(x)|^2).
\end{aligned}$$

The integration over α can then be performed, replacing the first parenthesis by

$$\left(\ln \left(\frac{q^2}{\pi^2 T^2} \right) - 2 + 2\gamma \right). \quad (4.20)$$

If this is added to the zero temperature result (4.9) the term $\ln(q^2/m_F^2) - 2$ in this equation gets replaced by $\ln(T^2/m_F^2) + 2\ln \pi - 2\gamma$. This term appears in the high temperature potential in λ_T .

Collecting from Eqs. (4.9) and (4.17) the terms which have not yet been included into the high temperature potential we find the following renormalized contribution of the first and second order Feynman graphs:

$$\begin{aligned} \Delta S_{\text{ren}}^{(1+2)}(\Phi, T) &= -3\beta \frac{m_t^4}{16\pi^2} \int \frac{d^3q}{(2\pi)^3} \left(|\widetilde{\Phi}^2(q)|^2 + \frac{q^2}{m_t^2} |\widetilde{\Phi}(q)|^2 \right) \\ &\quad \left(\ln \left(\frac{q^2}{m_t^2} \right) - 2 + 4 \int_0^1 d\alpha \int_0^\infty \frac{dp}{E_\alpha} \frac{1}{\exp(E_\alpha/T) + 1} \right) \\ &\quad - 3\beta \frac{m_t^4}{16\pi^2} \ln \left(\frac{m_t^2}{a_F T^2} \right) \int \frac{d^3q}{(2\pi)^2} |\widetilde{\Phi}^2(q)|^2 . \end{aligned} \quad (4.21)$$

Here we have taken into account the color factor 3, we have replaced m_F by m_t and we have replaced the formal x integration by a q integration in order to deal with the q dependence of the kernels correctly. Note that $\Phi^4(x)$ becomes here the square of the Fourier transform of Φ^2 .

5 Calculation of the finite part of the effective action

What remains to be evaluated is the sum of all Feynman graphs of order 3 and higher. This contribution is finite, we denote it as $S_{\text{eff}}^{(3)}(\phi)$. We present an exact numerical computation, using a general theorem on functional determinants [29] and an analytic approximation based on the gradient expansion. The results of the two methods will be compared at the end of this section.

5.1 Numerical computation

As mentioned above the fermionic one-loop effective action at finite temperature can be written - including the color factor 3 - as

$$S_{\text{eff}} = -\frac{3}{2} \sum_{n=-\infty}^{\infty} \ln \det \left(\frac{-\Delta + \nu_n^2 + \mathcal{V}}{-\Delta + \nu_n^2} \right) = -3 \sum_{n=0}^{\infty} \ln \mathcal{J}(\nu_n). \quad (5.1)$$

As the background field is spherically symmetric the determinant can be decomposed into its partial wave contributions. This is readily done by introducing the usual spinors for given j and $l = j \pm 1/2$ as given in the textbook of Bjorken and Drell [30]. One finds then

$$S_{\text{eff}} = - \sum_{n=0}^{\infty} \sum_{l=0}^{\infty} 6(2l+1) \ln \mathcal{J}_l(\nu_n). \quad (5.2)$$

Here the the partial wave determinants $\mathcal{J}_l(\nu)$ are defined as

$$\mathcal{J}_l(\nu) = \det \left(\frac{\mathbf{M}_1 + \nu^2}{\mathbf{M}_1^0 + \nu^2} \right)$$

with the partial wave fluctuation operators

$$\begin{aligned} \mathbf{M}_1 &= \mathbf{M}_1^0 + \mathbf{V}(r) \\ \mathbf{M}_1^0 &= -\mathbf{1} \left(\frac{d^2}{dr^2} + \frac{2}{r} \frac{d}{dr} \right) + \frac{1}{r^2} \begin{Bmatrix} l(l+1) & 0 \\ 0 & (l+1)(l+2) \end{Bmatrix} \end{aligned} \quad (5.3)$$

$$\mathbf{V}(r) = \begin{Bmatrix} m^2(r) & dm(r)/dr \\ dm(r)/dr & m^2(r) \end{Bmatrix}. \quad (5.4)$$

A very fast method for computing fluctuation determinants is based on a theorem on functional determinants [29] which can be generalized to a coupled ($n \times n$) system:

Let $\mathbf{f}(\nu, r)$ and $\mathbf{f}^0(\nu, r)$ denote the ($n \times n$) matrices formed by n linearly independent solutions $f_i^\alpha(\nu, r)$ and $f_i^{\alpha 0}(\nu, r)$ of

$$\left(\mathbf{M}_1 + \nu^2 \right)_{ij} f_j^\alpha(\nu, r) = 0 \quad (5.5)$$

and

$$\left(\mathbf{M}_1^0 + \nu^2 \right)_{ij} f_j^{\alpha 0}(\nu, r) = 0 \quad (5.6)$$

respectively, with regular boundary conditions at $r = 0$. Here the latin lower index denotes the n components while the different solutions are labelled by the Greek upper index. Let these solutions be normalized in such a way that

$$\lim_{r \rightarrow 0} \mathbf{f}(\nu, r) \left(\mathbf{f}^0(\nu, r) \right)^{-1} = \mathbf{1}. \quad (5.7)$$

Then the statement of the theorem is:

$$\mathcal{J}_l(\nu) \equiv \frac{\det(\mathbf{M}_1 + \nu^2)}{\det(\mathbf{M}_1^0 + \nu^2)} = \lim_{r \rightarrow \infty} \frac{\det \mathbf{f}(\nu, r)}{\det \mathbf{f}^0(\nu, r)}. \quad (5.8)$$

Here the determinants on the left-hand side are determinants in functional space while those on the right-hand side are ordinary determinants of the $n \times n$ matrices defined above. The theorem already has been applied to the calculation of the one-loop effective action of a single scalar field on a bubble background in [27, 18] and of a fermion system at temperature $T = 0$ on a similar background in [31] which we refer to for more technical details.

In the numerical application the solutions f_k^α are written as [32]

$$f_k^\alpha(\nu, r) = (\delta_k^\alpha + h_k^\alpha(\nu, r)) i_{l_k}(\nu r) \quad (5.9)$$

with the boundary condition $h_k^\alpha(\nu, r) \rightarrow 0$ as $r \rightarrow 0$. Of course the value l_k depends on the channel. This way one generates a set of linearly independent solutions which near $r = 0$ behave like the free solution as required by the theorem which then takes the form

$$\mathcal{J}(\nu) = \lim_{r \rightarrow \infty} \det(\delta_k^\alpha + h_k^\alpha(\nu, r)). \quad (5.10)$$

The functions $h_k^\alpha(\nu, r)$ satisfy the differential equation

$$\frac{d^2}{dr^2} h_k^\alpha(\nu, r) + 2 \left(\frac{1}{r} + \nu \frac{i'_{l_k}(\nu r)}{i_{l_k}(\nu r)} \right) \frac{d}{dr} h_k^\alpha(\nu, r) = V_{kk'}(r) \left(\delta_{k'}^\alpha + h_{k'}^\alpha(\nu, r) \right) \frac{i_{l_{k'}}(\nu r)}{i_{l_k}(\nu r)}. \quad (5.11)$$

This equation can easily be used for generating the functions h_k^α order by order in the potential V . Introducing the contribution of order k in the potential as $\mathbf{h}^{(k)}$ and defining $\overline{\mathbf{h}^{(k)}}$ via

$$\overline{\mathbf{h}^{(k)}} \equiv \sum_{j=k}^{\infty} \mathbf{h}^{(j)}$$

as in [31], the relevant contribution $S_{\text{eff}}^{(3)}$ is found to be

$$S_{\text{eff}}^{(3)} = - \sum_{n=0}^{\infty} \mathcal{K}^{(3)}(\nu_n), \quad (5.12)$$

where

$$\begin{aligned} \mathcal{K}^{(3)}(\nu) &= \sum_{l=0}^{\infty} 6(2l+1) \lim_{r \rightarrow \infty} \left\{ \ln \det \left(\mathbf{1} + \overline{\mathbf{h}^{(1)}}(\nu, r) \right) \right. \\ &\quad \left. - \text{tr} \left(\mathbf{h}^{(1)}(\nu, r) + \mathbf{h}^{(2)}(\nu, r) - \frac{1}{2} \left[\mathbf{h}^{(1)}(\nu, r) \right]^2 \right) \right\}. \end{aligned} \quad (5.13)$$

The expression $\mathcal{K}^{(3)}(\nu)$ was evaluated by summing the partial waves computed numerically up to $l_{\text{max}} = 30$ extrapolated for higher values of l using an Ansatz $al^{-5} + bl^{-6} + cl^{-7}$. The asymptotic behaviour is supposed to set in at values of $l \gg \nu R$ where R is the typical radius of the bubble. Since R has typical values of 20-40, this means that for our l_{max} the extrapolation becomes unreliable already for ν of order 1. We will discuss this point again below.

5.2 Analytic approximation using the gradient expansion

In [31] an approximation of the gradient expansion type has been given for the one-loop effective action at zero temperature for the case of a massive fermion with Yukawa coupling to an external scalar field. The calculation to be done here is similar because the Matsubara frequency ν_n enters in the same way as a mass term and so the structure of the determinant is of the same type.

The logarithm of the determinant $\mathcal{J}(\nu)$ can be written exactly as

$$\ln \mathcal{J}(\nu) = \text{Tr} \ln (\mathbf{1} + \mathbf{G}_0 \mathcal{V}) \quad (5.14)$$

where the free Green function \mathbf{G}_0 is defined by

$$(\mathbf{M} + \nu^2) \mathbf{G}_0 = \mathbf{1}. \quad (5.15)$$

Defining the Fourier transform of the potential \mathcal{V} as

$$\tilde{\mathcal{V}}(\mathbf{q}) = \int d^3x \mathcal{V}(\mathbf{x}) \exp(-i\mathbf{q}\mathbf{x}) \quad (5.16)$$

the fluctuation determinant can be expanded as

$$\ln \mathcal{J}(\nu) = \sum_{k=1}^{\infty} \text{tr} \frac{(-1)^{k+1}}{k} \int \frac{d^3p}{(2\pi)^3} \prod_{j=1}^k \int \frac{d^3q_j}{(2\pi)^3} \frac{\tilde{\mathcal{V}}(\mathbf{q}_j)}{(\mathbf{p} + \mathbf{Q}_j)^2 + \nu^2} (2\pi)^3 \delta^{(3)}(\mathbf{Q}_k) \quad (5.17)$$

where

$$\mathbf{Q}_j = \sum_l^j \mathbf{q}_l.$$

Expanding the denominators including terms up to order ν^{-2k-4} we get

$$\prod_{j=1}^k \frac{1}{(\mathbf{p} + \mathbf{Q}_j)^2 + \nu^2} \simeq \frac{1}{(\mathbf{p}^2 + \nu^2)^k} \left[1 - \sum_{l=1}^k \frac{\mathbf{Q}_l^2}{(\mathbf{p}^2 + \nu^2)} + \frac{4}{3} \frac{\mathbf{p}^2}{(\mathbf{p}^2 + \nu^2)^2} \left(\sum_{l>l'} \mathbf{Q}_l \mathbf{Q}_{l'} + \sum_{l=1}^k \mathbf{Q}_l^2 \right) \right]. \quad (5.18)$$

As the potential is $\mathcal{V} = m_F^2 \Phi^2 + m_F \gamma \nabla \Phi$ we have

$$\text{tr} \prod_{j=1}^k \tilde{\mathcal{V}}(\mathbf{q}_j) \simeq 4m_F^{2k} \left[\prod_{j=1}^k \tilde{\Phi}^2(\mathbf{q}_j) - \frac{1}{m_F^2} \sum_{l>l'} \mathbf{q}_l \mathbf{q}_{l'} \tilde{\Phi}(\mathbf{q}_l) \tilde{\Phi}(\mathbf{q}_{l'}) \prod_{j \neq l, l'} \tilde{\Phi}^2(\mathbf{q}_j) \right]. \quad (5.19)$$

After inserting these expansions in (5.17) and transforming back to x -space the remaining integrations (except of one space integration) and the k -summation can be done. Of course we have to omit those terms which are divergent. As we are working in four dimensions these are the terms with $k = 1$ and $k = 2$, they have been discussed in the previous section.

Our final result written in the form of $\mathcal{K}(\nu) = 3 \ln \mathcal{J}(\nu)$ is

$$\begin{aligned} \mathcal{K}^{(3)}(\nu) \simeq & \frac{3\nu^3}{2\pi} \int d^3x \left\{ -\frac{4}{3} \left[\left(1 + \frac{m_F^2 \Phi^2}{\nu^2} \right)^{\frac{3}{2}} - 1 - \frac{3}{2} \frac{m_F^2 \Phi^2}{\nu^2} - \frac{3}{8} \frac{m_F^4 \Phi^4}{\nu^4} \right] \right. \\ & \left. + \frac{m_F^2 (\nabla \Phi)^2}{2\nu^4} \left[\left(1 - \left(1 + \frac{m_F^2 \Phi^2}{\nu^2} \right)^{-\frac{1}{2}} \right) - \frac{m_F^2 \Phi^2}{3\nu^2} \left(1 - \left(1 + \frac{m_F^2 \Phi^2}{\nu^2} \right)^{-\frac{3}{2}} \right) \right] \right\}. \end{aligned} \quad (5.20)$$

This expression has to be evaluated using for Φ the numerical bubble profiles. The accuracy is only limited by the accuracy of these profiles and by that of the

numerical integration. With our numerical precision the results are reliable to at least 6 significant digits.

The approximate results for $\overline{\mathcal{K}^{(3)}}$ can be compared with the exact numerical ones computed using (5.13). For the purpose of comparison we treat ν as a continuous parameter. We display the exact and approximate results in Figs. 1 and 2 for two typical bubble profiles, a small bubble with $y = 0.6$ and a large bubble corresponding to $y = 0.3$ (see (2.19) for the definition of y). The analytic approximation is seen to describe the trend of the exact results over the whole range. The gradient expansion is expected to converge at large ν . This expectation is substantiated by the exact numerical results in the region where they are reliable. It is seen, however, that the exact results start dropping off at values of $\nu \simeq 1 - 2$; as mentioned above this is related to the fact that the convergence of the partial wave summation becomes poorer with increasing ν . Since the values of ν relevant for the Matsubara frequency summation (5.12) are $\nu \geq \pi T \approx 9$ (in our units $g\tilde{\nu}$) we have to rely on the gradient expansion in computing the finite temperature effective action.

6 Results

We have computed the finite temperature fermionic effective action for Higgs masses of 60, 70 and 80 GeV and for top quark masses $m_t = 160, 170$ and 180 GeV. These results are given in Tables 1 to 3. As mentioned in section 2 we have considered only the contribution of the top quark since lighter quarks and leptons will give negligible contributions. Their contribution has already been dismissed in the basic high temperature action (2.1) and including them would be inconsistent.

For each set of mass parameters we have determined the bubble profiles for various values of the variable y defined in (2.19); y determines the temperature and the bubble action. We give separately the renormalized first and second order contributions $\Delta S_{\text{ren}}^{(1+2)}$, Eq. (4.21) determined in section 3 and the finite sum of all higher order contributions $S_{\text{eff}}^{(3)}$ whose computation was discussed in the previous section. It is given by the analytic expression Eq. (5.20), inserted into the Matsubara sum (5.12). The total one-loop effective action, reduced by the terms included already in the ‘classical’ effective potential is given, of course, by the sum $\Delta S_{\text{eff}}^{(1+2)} + S_{\text{eff}}^{(3)}$.

The fermion determinant is seen to yield a negative contribution to the effective action, which means that bubble nucleation is enhanced by this contribution (cf. Eqs. (2.10) and (2.11)). It is interesting to analyze the relative importance of the various contributions. The $\overline{(3)}$ part given in Eq. (5.20) is relatively small, also the zero-derivative part of the leading order (1 + 2) contributions in Eq. (4.21). This is not unexpected, as the zero-derivative part was already included into the

effective potential, so its leading first and second order contributions are subtracted. The dominant contribution is the gradient term in Eq. (4.21), the finite part of the wave function renormalization. It is also displayed in Tables 1 to 3 in the columns labelled $\Delta_{\text{grad}}^{(1+2)}$. This means that the top quark contribution can be described, essentially, by local terms in analytic form: those already contained in the effective potential and the finite part of the wave function renormalization; this is very convenient because these terms can be incorporated into the basic action from which the bubble profile is computed. If this is done, the remaining corrections can be expected to be very small. In a selfconsistent determination of the bubble profiles such an action can be expected to yield an excellent first approximation.

References

- [1] see ‘Electroweak physics and the Early Universe’ Eds. F. Freire and J. Romão, Plenum Publ. Corp., N. Y., 1994, for a recent account of the state of art.
- [2] V. Kuzmin, V. Rubakov and M. Shaposhnikov, Phys. Lett. **B155**, 36 (1985).
- [3] for a review see A. Cohen, D. Kaplan and A. Nelson, Ann. Rev. Nucl. Part. Sci. **43**, 27 (1993).
- [4] G. Farrar and M. Shaposhnikov, Phys. Rev. Lett. **70**, 2833 (1993), **71**, 210(E) (1993), CERN preprints CERN-TH 6732-93 and CERN-TH 6734-93.
- [5] M. B. Gavela, M. Lozano, J. Orloff and O. Pene, Nucl. Phys. **B430**, 345 (1994); M. B. Gavela, P. Hernandez, J. Orloff, O. Pene and C. Quimbay, Nucl. Phys. **B430**, 382 (1994).
- [6] W. Buchmüller, Z. Fodor, T. Helbig and D. Walliser, Ann. Phys. **234**, 260 (1994).
- [7] K. Farakos, K. Kajantie, K. Rummukainen and M. Shaposhnikov, Nucl. Phys. **B425**, 67 (1994).
- [8] K. Kajantie, K. Rummukainen and M. Shaposhnikov, Nucl. Phys. **B407**, 356 (1993).
- [9] Z. Fodor, J. Hein, K. Jansen, A. Jaster, I. Montvay and F. Czikor, Phys. Lett. **B334**, 405 (1994).
- [10] K. Farakos, K. Kajantie, K. Rummukainen and M. Shaposhnikov, Phys. Lett. **B336**, 494 (1994).
- [11] M. S. Turner, E. J. Weinberg and L. M. Widrow, Phys. Rev. **D46**, 2384 (1992).
- [12] B. H. Liu, L. McLerran and N. Turok, Phys. Rev. **D46**, 2688 (1992).
- [13] M. Dine, R. G. Leigh, P. Huet, A. Linde and D. Linde, Phys. Rev. **D46**, 550 (1992).
- [14] J. S. Langer, Ann. Phys. (N. Y.) **41**, 108 (1967); *ibid.* **54**, 258 (1969).
- [15] S. Coleman, Phys. Rev. **D15**, 2929 (1977).
- [16] G. Callan and S. Coleman, Phys. Rev. **D16**, 1762 (1977).
- [17] J. Krippfganz, A. Laser and M. G. Schmidt, Nucl. Phys. **B433**, 467 (1995).
- [18] J. Baacke, Preprint DO-TH-95/04, March 1995.

- [19] D. Dyakonov, M. Polyakov, P. Sieber, J. Schaldach and K. Goeke, Phys. Rev. **D49**, 6964 (1994).
- [20] S. Coleman and E. Weinberg, Phys. Rev. **D7**, 1888 (1973).
- [21] D. A. Kirshnits and A. D. Linde, Ann. Phys. (N.Y.) **101**, 195 (1976).
- [22] M. E. Shaposhnikov, Nucl. Phys. **B287**, 757 (1987); *ibid.* bf B 299, 581 (1987).
- [23] G. W. Anderson and L. J. Hall, Phys. Rev. **D45**, 2685 (1991).
- [24] E. J. Weinberg, Phys. Rev. **D47**, 4614 (1993).
- [25] I. Affleck, Phys. Rev. Lett. **46**, 388 (1981).
- [26] A. D. Linde, Nucl. Phys. **B216**,421 (1983).
- [27] J. Baacke and V. G. Kiselev, Phys. Rev. **D48**, 5648 (1993).
- [28] L. Dolan and R. Jackiw, Phys. Rev. **D9**, 3320 (1974).
- [29] see e. g. S. Coleman, *The Uses of Instantons*, in *The Aspects of Symmetry*, Cambridge University Press 1985.
- [30] J. D. Bjorken and S. Drell, *Relativistic Quantum Mechanics*, McGraw-Hill Book Company, New York 1964.
- [31] J. Baacke, H. So and A. Suerig, Z. Phys. **C63**, 689 (1994).
- [32] J. Baacke, Z. Phys. **C53**, 407 (1992).

Table Captions

Table 1 Corrections to the effective action at finite temperature for $m_H = 60$ GeV. ϵ and y are defined in Eq. (2.14) and (2.19); $\Delta S_{\text{ren}}^{(1+2)}$ is defined by Eqs. (4.21), $\Delta S_{\text{grad}}^{(1+2)}$ is the gradient part as explained in section 6; $\overline{S^{(3)}}$ is given by Eqs. (5.12) and (5.20); \tilde{S} , the classical action of Eq. (2.16) is given for comparison.

Table 2 Corrections to the effective action at finite temperature for $m_H = 70$ GeV. Definitions as in Table 1.

Table 3 Corrections to the effective action at finite temperature for $m_H = 80$ GeV. Definitions as in Table 1.

Figure Captions

Fig. 1 The loop expansion of the effective action. The lines represent the propagators and the dots indicate the vertices $V(x)$.

Fig. 2 Results of the numerical computation compared to the analytic approximation for $y = 0.3$, $m_H = 60$ GeV and $m_t = 170$ GeV. The dots interpolated by a dotted line represent the numerical results, the solid line is the analytic approximation of Eq. (5.13)

Fig. 3 The same as Figure 2 for $y = 0.6$.

m_t [GeV]	T [GeV]	ϵ	y	$\Delta S_{\text{ren}}^{(1+2)}$	$\Delta S_{\text{grad}}^{(1+2)}$	$\overline{S_{\text{eff}}^{(3)}}$	\tilde{S}
160	94.894	1.867	0.2	-23.160	-23.250	-18.923	308.02
	94.854	1.800	0.3	-9.637	-9.753	-3.774	132.30
	94.682	1.600	0.6	-1.685	-1.693	-0.0781	24.847
170	94.5288	1.867	0.2	-23.752	-23.695	-20.418	278.47
	94.495	1.800	0.3	-9.973	-10.091	-4.184	121.40
	94.347	1.600	0.6	-1.734	-1.742	-0.0854	22.686
180	94.6605	1.867	0.2	-24.558	-24.291	-20.929	251.60
	94.631	1.800	0.3	-10.002	-10.114	-4.110	107.27
	94.5056	1.600	0.6	-1.757	-1.766	-0.0855	20.245

Table 1

m_t [GeV]	T [GeV]	ϵ	y	$\Delta S_{\text{ren}}^{(1+2)}$	$\Delta S_{\text{grad}}^{(1+2)}$	$\overline{S_{\text{eff}}^{(3)}}$	\tilde{S}
160	106.015	1.867	0.2	-18.933	-18.740	-6.746	217.14
	105.980	1.800	0.3	-7.956	-8.006	-1.384	94.690
	105.826	1.600	0.6	-1.387	-1.391	-0.0282	17.630
170	104.7850	1.867	0.2	-20.091	-19.899	-8.412	207.39
	104.7545	1.800	0.3	-8.438	-8.500	-1.726	90.411
	104.6202	1.600	0.6	-1.470	-1.475	-0.0352	16.830
180	104.094	1.867	0.2	-20.897	-20.743	-9.602	193.72
	104.0674	1.800	0.3	-8.751	-8.799	-1.946	83.921
	103.951	1.600	0.6	-1.522	-1.528	-0.0396	15.632

Table 2

m_t [GeV]	T [GeV]	ϵ	y	$\Delta S_{\text{ren}}^{(1+2)}$	$\Delta S_{\text{grad}}^{(1+2)}$	$S_{\text{eff}}^{(3)}$	\tilde{S}
160	117.541	1.867	0.2	-15.433	-15.177	-2.512	156.45
	117.510	1.800	0.3	-6.483	-6.483	-0.514	68.050
	117.374	1.600	0.6	-1.136	-1.139	-0.0107	12.708
170	115.4848	1.867	0.2	-16.747	-16.411	-3.388	153.28
	115.4573	1.800	0.3	-6.985	-6.984	-0.688	66.460
	115.337	1.600	0.6	-1.222	-1.225	-0.0142	12.410
180	114.0042	1.867	0.2	-17.696	-17.287	-4.163	146.18
	113.9801	1.800	0.3	-7.387	-7.386	-0.852	63.649
	113.874	1.600	0.6	-1.287	-1.290	-0.0174	11.846

Table 3

$$S_{\text{eff}} = -\frac{1}{2} \text{ (circle with 1 dot) } + \frac{1}{4} \text{ (circle with 2 dots) } - \frac{1}{6} \text{ (circle with 3 dots) } + \dots$$

Figure 1

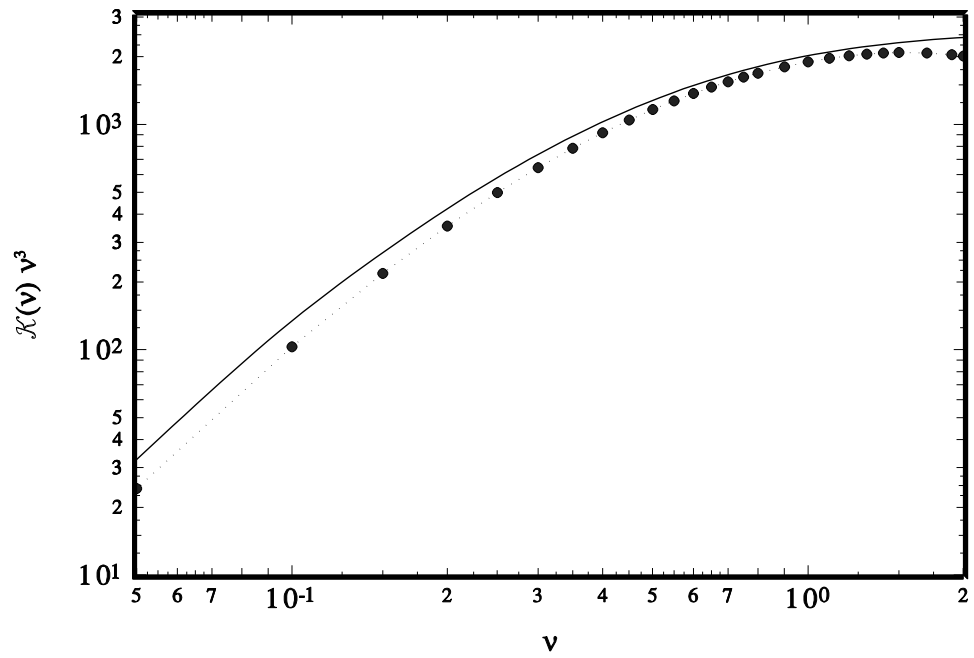


Figure 2

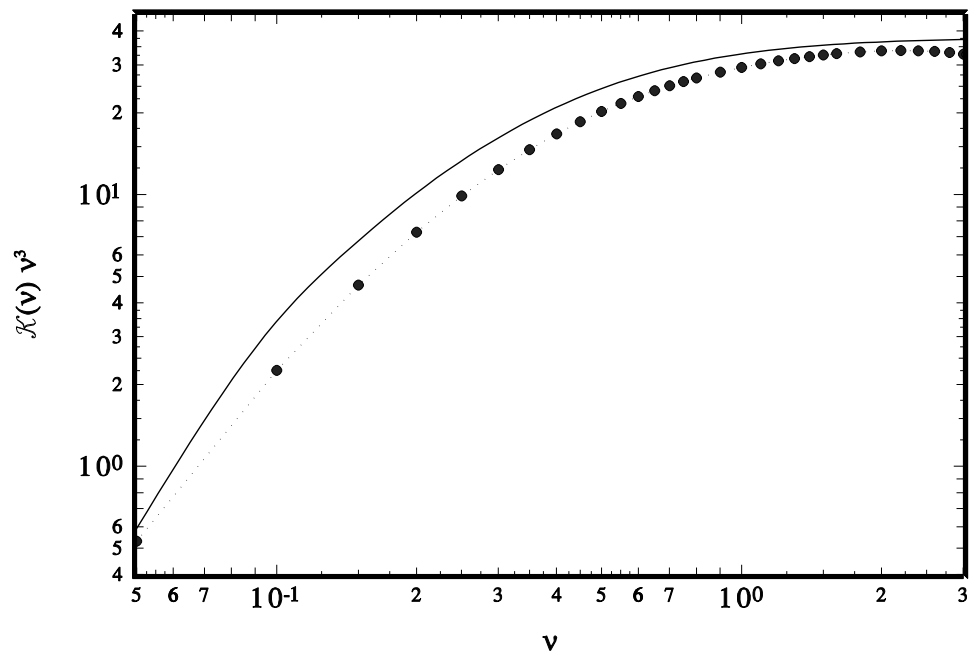


Figure 3